

VIBRATION TRANSMISSIBILITY OF LOW FREQUENCY ISOLATOR

TRUYỀN DAO ĐỘNG CỦA BỘ CÁCH LY TẦN SỐ THẤP

Le Thanh Danh, Nguyen Vu Anh Duy

Ho Chi Minh City University of Technology, Vietnam

Received 26/10/2016, Peer reviewed 11/11/2016, Accepted for publication 25/11/2016

ABSTRACT

It is known that the quality of a vibration isolation system can be improved by reducing the stiffness of the system. However, in this way, the load supporting capacity of isolator cannot be maintained. In order to eliminate the dichotomy between the load bearing capacity and the reduction in stiffness, this paper will introduce a low frequency vibration isolator. First, the relationship between the configurative parameters and the dynamic stiffness of the isolator is obtained. Then, the characteristic of the motion transmissibility of the system at the steady state is analyzed through the normal form solution (NF). From this analysis result, the curve of the vibration transmission is predicted. The simulation results confirm that the isolation effectiveness of this model is better than that of the traditional model when the dimensionless dynamic stiffness at the equilibrium position is lower than one and bigger than zero or equal to zero. Besides, these results furnish a useful insight for the design of the low frequency vibration isolation model.

Keywords: Isolator; Low dynamic stiffness; Normal form; Vibration transmissibility; Steady state vibration.

TÓM TẮT

Như đã biết, chất lượng của một bộ cách ly có thể được nâng cao bằng phương pháp giảm độ cứng của hệ thống. Tuy nhiên, nếu độ cứng giảm thì khả năng đỡ tải của bộ cách ly không được duy trì. Vì vậy, để khắc phục mâu thuẫn giữa khả năng đỡ tải và giảm độ cứng, bài báo này sẽ giới thiệu một mô hình bộ cách ly dao động tần số thấp. Đầu tiên, mối quan hệ giữa thông số cấu hình và độ cứng động học của hệ thống được trình bày. Sau đó, đặc tính truyền dao động của bộ cách ly được phân tích bằng phương pháp normal form. Từ kết quả phân tích này, đường cong truyền dao động của bộ cách ly được dự đoán. Kết quả mô phỏng số cho thấy rằng: khi độ cứng động học không thứ nguyên tại vị trí cân bằng tĩnh nhỏ hơn một và lớn hơn hoặc bằng không thì hiệu quả cách ly dao động của bộ cách ly tần số thấp tốt hơn bộ cách ly truyền thống. Ngoài ra, kết quả phân tích này rất hữu ích cho việc thiết kế bộ cách ly dao động tần số thấp.

Từ khóa: Bộ cách ly; Độ cứng động học thấp; Normal form; Truyền dao động; Dao động bình ổn.

1. INTRODUCTION

The conventional passive vibration isolator, which is widely used for controlling

unwanted vibration, consists of a linear stiffness spring, K , in parallel to a damper, C [1,2]. Vibration attenuation is obtained for input frequencies greater than $\sqrt{2}$ times

the natural frequency of the isolation system. For input frequencies below $\sqrt{2}$ times the natural frequencies and especially those close to the natural frequency, the vibration level of the isolated equipment is actually increased, as compared with that of the base. In order to extend the isolation region toward the ultra-low excitation frequencies, the stiffness of spring K is mostly employed to reduce the natural frequency of the system, especially from 0.5 to 5 Hz, in which the vibration is harmful and dangerous to humans, and has been investigated by many researchers [3]. This idea indicates that the stiffness of the system is decreased. However, the reduction in stiffness leads to a large static deformation and a low bearing capacity. So, this isolator only offers a good effect with high excitation frequencies. Many papers and reports have given solutions to reduce the resonance frequency, such as using a highly deformed elastic structure working as a nonlinear spring to support a static load [4-7] or another structure that is also based on the elastic model with extreme geometric nonlinearity [8-9]. The purpose of elastic structures is to reduce the resonance frequency. However, these structures easily lose stability and their low load bearing capacity when the stiffness of the elastic elements is very low

In this paper, an isolator is introduced for isolating low frequency vibrations. Then, Normal form method is used to predict the curve of vibration transmissibility of this isolator. This paper is organized as follows. The mathematical model of system is presented in section 2. In section 3, the vibration transmissibility is presented. The numerical simulation results are shown in section 4. Finally, some conclusions are drawn in section 5.

2. MECHANICAL MODEL OF LOW FREQUENCY VIBRATION ISOLATION

Figure 1 introduces a low frequency vibration isolation model. In which, the isolation object is supported by a vertical spring. The dynamic stiffness of this system is reduced by using two horizontal springs. Initially, at the static equilibrium position presented by the dashed line, the mass is held in equilibrium by the compression force of the vertical spring F_v and the gravity force Mg which is opposite of the force F_v

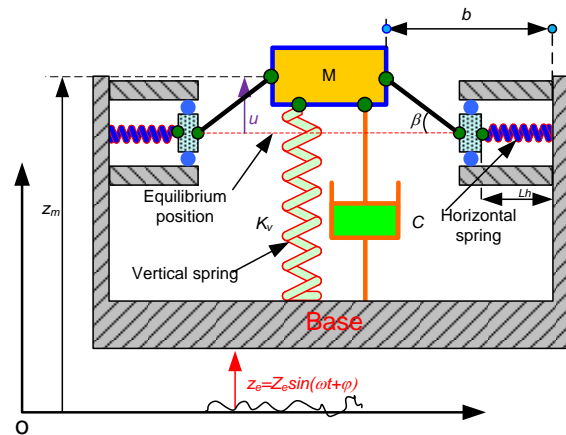


Figure 1. Mechanical model

3. Vibration transmissibility

3.1 Dynamic equation

If an excitation z_e having the frequency ω is transmitted from base the isolation object, hence the isolation object is moved away from the equilibrium position, u as shown

The vertical restoring force is written as:

$$\hat{F} = (h_{id} - \hat{u}) + 2\alpha \left(\frac{1}{\sqrt{\gamma_1^2 - \hat{u}^2}} - \frac{\gamma_2}{\sqrt{\gamma_1^2 - \hat{u}^2}} + 1 \right) \hat{u} \quad (1)$$

where: $\gamma_1 = \frac{a}{L_o}$, $\gamma_2 = \frac{b}{L_o}$, $\alpha = \frac{K_h}{K_v}$, $\hat{u} = \frac{a}{L_o}$;

K_h, K_v are horizontal and vertical spring stiffness, respectively. L_o is the original

length of the horizontal spring. h_{id} is the initial deformation of the vertical spring. b is the distance from the wall to the isolation mass. M is the weight of the isolation object.

From Eq. (1), the dimensionless dynamic stiffness of the system is described as following:

$$\hat{K} = 1 + 2\alpha \left(\frac{\hat{u}^2 (\gamma_2 - 1)}{(\gamma_1^2 - \hat{u}^2)^{3/2}} - \frac{(1 - \gamma_2) + \sqrt{\gamma_1^2 - \hat{u}^2}}{\sqrt{\gamma_1^2 - \hat{u}^2}} \right) \quad (2)$$

Eq. (1) expresses the restoring force of the system as a function of the configurative parameters γ_1 , γ_2 , α and the displacement, x . As in Fig. 2, it can be seen that the shape of the original restoring force curve (denoted by solid line) is similar to the third-order curve. Thus, the third-order function is used for expressing the approximation of the dimensionless restoring force of the system.

Generally, a smooth function can be expressed by expanding Taylor series up to the order N as

$$f(\hat{x}) = f(\hat{x}_o) + \sum_{n=1}^N \frac{f^n(\hat{x}_o)}{n!} (\hat{x} - \hat{x}_o)^n \quad (3)$$

Here, the system is designed for the desirable vibration with the small amplitude about the static equilibrium position. Hence, the function of the dimensionless restoring force is expanded around this position. By ignoring the high-order term, the approximate equation of the dimensionless restoring force is given as

$$F_{ap} = h_{id} K_v + K_v \left(1 - 2\alpha \frac{1 - \gamma_2 + \gamma_1}{\gamma_1} \right) u + \alpha K_v \frac{\gamma_2 - 1}{\gamma_1^3 L_o^2} u^3 \quad (4)$$

As shown in Fig. 2, if the vibration of the system is around the static equilibrium position, the approximate curve of the restoring force (depicted by dashed line)

nearly coincides with the curve of the exact expression. Therefore, the third-order approximate function can be used for analyzing the dynamic of the system in the static equilibrium position.

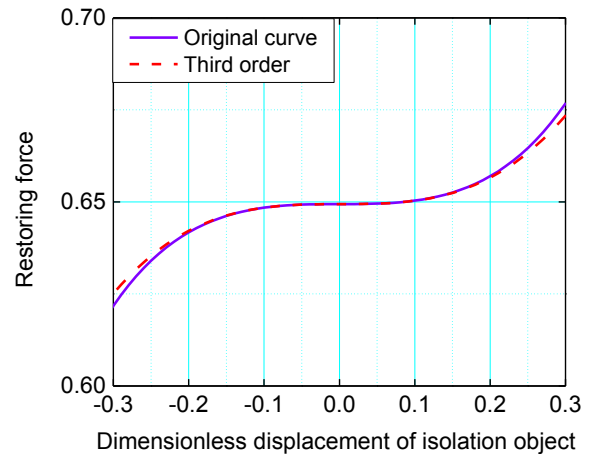


Figure 2. Comparison of the approximate with the exact expressions

Applying the Lagrange's Equation, the motion equation is obtained as following:

$$\ddot{u} + \frac{C}{M} \dot{u} + \frac{K_v}{M} \left(1 - 2\alpha \frac{1 - \gamma_2 + \gamma_1}{\gamma_1} \right) u + \alpha \frac{\gamma_2 - 1}{\gamma_1^3} \frac{K_v X^2}{ML_o^2} u^3 = Z_e \omega^2 \cos(\omega t) \quad (5)$$

In term of these dimensionless parameters, Eq. (5) can be rewritten as bellow

$$\hat{u}'' + 2\xi \hat{u}' + \omega_n^2 \hat{u} + \eta \hat{u}^3 = \Omega^2 \cos(\Omega \tau + \phi) \quad (6)$$

where:

$$\hat{u} = \frac{u}{Z_2}, \xi = \frac{C}{2M\omega_n}, \omega_n^2 = \frac{K_v}{\omega_n^2 M} \left(1 - 2\alpha \frac{1 - \gamma_2 + \gamma_1}{\gamma_1} \right), \eta = \alpha \frac{K_v X^2}{\omega_n^2 M L_o^2} \frac{\gamma_2 - 1}{\gamma_1^3}$$

Eq. (6) is the approximate dynamic equation that expresses the steady state vibration of the isolated object around the equilibrium position with the small amplitude. It is well-know nonlinear vibration equation "called Duffing's equation". As is known, the solution of the system consists of two parts: a particular solution and a homogeneous solution (free vibration term). Here, positive

damping, hence the free vibration term will die away in time. The resulting response is called the steady state response and it only consists of the particular solution. The steady state response has the same frequency as the excitation, but that phase is shifted from that of the excitation an amount that depends on the damping

3.2 Normal Form method

Here, the Normal form method (NF) is employed to find the steady state solution of the system for each of the certain excitation frequency. The method transforms Eq. (6) to the form:

$$\ddot{\hat{v}} + \omega^2 \hat{v} + \Gamma_{\hat{v}} = P_{\hat{v}} x r \quad (7)$$

here: $\hat{u} = \hat{v} + [e]r$,

$$\Gamma_{\hat{v}}(\hat{v}, r) = \varepsilon f(\hat{v}, r) = \varepsilon (2\xi' \dot{\hat{v}} + \eta' \hat{v}^3) \text{ and } P_{\hat{v}} = P_{\hat{u}}$$

$$\xi' = \frac{\zeta}{\varepsilon}; \eta' = \frac{\eta}{\varepsilon} \text{ with } \varepsilon \text{ is small parameter}$$

Applying a nonlinear transform from v to w given by:

$$\hat{v} = \hat{w} + \varepsilon h(\hat{w}, r) \quad (8)$$

Eq. (7) is rewritten as following:

$$\ddot{\hat{w}} + \omega_n^2 \hat{w} + \Gamma_w(w, r) = P_w r; \quad (9)$$

here $\Gamma_w(w, r) = \varepsilon g(w, r)$

From Eqs.(7-9), we obtain as bellow:

$$\begin{aligned} \varepsilon^0 \quad P_w &= P_{\hat{v}} \\ \varepsilon^1 \quad g(\hat{w}, r) - \frac{d^2}{dt^2} h(\hat{w}, r) &= \omega_n^2 h(\hat{w}, r) + f(\hat{w}, r) \end{aligned} \quad (10)$$

The state vector \hat{w} is divided into components $\hat{w} = \hat{w}_1 + \hat{w}_2 = \frac{\hat{W}_1}{2} e^{i\Omega t} + \frac{\hat{W}_1}{2} e^{-i\Omega t}$

where \hat{W} is the amplitude of the state \hat{w} and

A vector \hat{w}^* matrix [A], [B] and [f] are defined so that satisfying Eq. (11)

$$\begin{aligned} f(\hat{w}, r) &= [f] \hat{w}^*(\hat{w}_1, \hat{w}_2, r) \quad (a) \\ g(\hat{w}, r) &= [A] \hat{w}^*(\hat{w}_1, \hat{w}_2, r) \quad (b) \\ h(\hat{w}, r) &= [B] \hat{w}^*(\hat{w}_1, \hat{w}_2, r) \quad (c) \end{aligned} \quad (11)$$

Combination of Eqs. (10, 11a) and the states vectors \hat{w}_1 and \hat{w}_2 we obtains as following:

$$\begin{aligned} \hat{w}^* &= [\hat{w}_1 \quad \hat{w}_2 \quad \hat{w}_1^3 \quad \hat{w}_1^2 \hat{w}_2 \quad \hat{w}_1 \hat{w}_2^2 \quad \hat{w}_2^3] \\ [f]^T &= [2\xi' \omega_n \Omega i \quad -2\xi' \omega_n \Omega i \quad \eta' \quad 3\eta' \quad 3\eta' \quad \eta'] \end{aligned}$$

The matrix [A] and [B] is determined by Eq. (12):

$$[f] - [A] = (-\Psi + (i\Omega)^2)[B] \quad (12)$$

where Ψ is found from following condition

$$\frac{d^2 \hat{w}^*(\hat{w}, r)}{dt^2} = \Psi \hat{w}^*(\hat{w}, r) \quad (13)$$

Finally, the matrixes [A] and [B] are expressed as following:

$$[A]^T = [2\xi' \omega_n i \Omega \quad -2\xi' \omega_n i \Omega \quad 0 \quad 3\eta_1' \quad 3\eta_1' \quad 0] \quad (14)$$

$$[B]^T = \left[0 \quad 0 \quad \frac{\eta'}{8\Omega^2} \quad 0 \quad 0 \quad \frac{\eta'}{8\Omega^2} \right] \quad (15)$$

Substitution of Eqs.(11-15) into Eq. (9) and transform from \hat{w} to \hat{u} , we have:

$$\begin{aligned} \left[(\omega_n^2 - \Omega^2) \hat{W} + \frac{3\eta}{4} \hat{W}^3 \right] \cos(\Omega t) - 2\xi' \omega_n \Omega \hat{W} \sin(\Omega t) \\ = \Omega^2 \cos(\Omega \tau) \cos(\phi) - \Omega^2 \sin(\Omega \tau) \sin(\phi) \end{aligned} \quad (16)$$

And steady-state solution is obtains as:

$$\hat{u} = \hat{W} \cos(\Omega t) + \left(\frac{\eta \hat{W}^3}{32\Omega^2} \right) \cos(3\Omega t) \quad (17)$$

From Eq. (16), we have:

$$(\hat{W}^2 - 1)\Omega^4 + 2(2\xi'^2 \omega_n^2 \hat{W}^2)\Omega^2 + \omega_n^2 \hat{W} + \frac{3\eta}{4} \hat{W}^3 = 0 \quad (18)$$

Then, the absolute vibration transmissibility (T_a) is defined as the ratio of the magnitude of the absolute displacement of the isolated object to the base as:

$$T_a = \frac{|z_m|}{|z_e|} = \frac{\sqrt{U^2 + Z_e^2 + 2UZ_e \cos \phi}}{Z_e} = \sqrt{\hat{U}^2 + 1 + \frac{2\hat{U}}{\Omega^2} \cos \phi} \quad (19)$$

4. NUMERICAL SIMULATION

4.1 Dynamic stiffness curve

Figure 3 shows the dynamic stiffness curve of the low frequency vibration isolation model with the configurative parameters $\gamma_1=0.75$, $\alpha=1$ and γ_2 within from 1.35 to 1.75. It can see that the dynamic stiffness curve is the concave parabola, on which the dynamic stiffness is minimum at the static equilibrium position. This stiffness will be increased according to the increase of the value of γ_2 . The dynamic stiffness of the system is greater or smaller than the vertical spring stiffness if $\gamma_2 \geq 1.75$ or $1.35 < \gamma_2 < 1.75$, respectively. If $\gamma_2 = 1.35$, the value of the dynamic stiffness at the equilibrium position is quasi-zero, this is the best case for isolating vibration. If $\gamma_2 < 1.35$, the system achieves the negative stiffness at the equilibrium position. This case, the system can not bear the load.

The relationship between the configurative parameters γ_1 , α and γ_2 , for which the dynamic stiffness at the equilibrium position is zero, is shown in Fig. 4

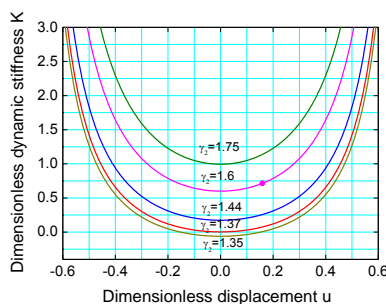


Figure 3. Dynamic stiffness curve

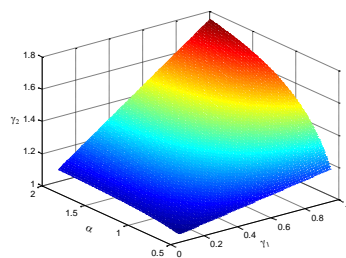


Figure 4. Relationship between the configurative parameters γ_1 , α và γ_2

4.2 Vibration transmissibility

Here, the configurative parameters of the system are also set up as following: $\gamma_1=0.75$, $\alpha=1$ and $1.35 \leq \gamma_2 \leq 1.75$. As above analyzed, the dynamic stiffness at the equilibrium position is reduced from one to zero according to the decrease in the value of γ_2 from 1.75 to 1.37. This leads to the expansion of the isolation region and the increase in the rate of the vibratory attenuation as presented in Fig. 5. Especially, if the dynamic stiffness at the equilibrium position is nearly equal to zero, the resonant peak and frequency are also reduced.

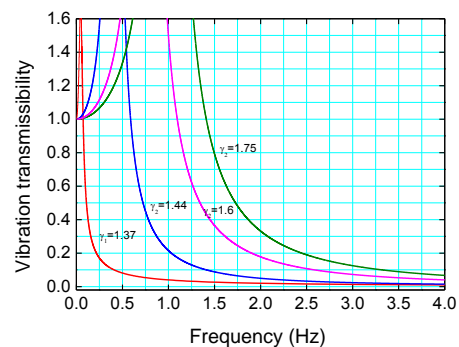


Figure 5. Vibration transmissibility curve

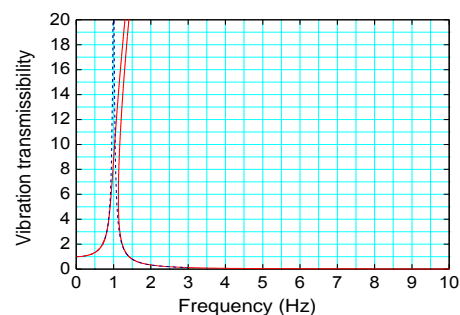


Figure 6. Isolation effectiveness comparison

In addition, the comparison of the vibration transmissibility between the low frequency vibration isolator having $\gamma_2=1.75$ and the traditional isolation model is considered as shown in Fig. 6. The both systems have the same vertical spring but the traditional system is absent two horizontal springs. The result is that the both systems offer the same frequency region of isolation.

This is evident because with this configurative parameter, the dynamic stiffness at the equilibrium position of the low frequency isolation system is nearly equal to the stiffness of the vertical spring

Correspondingly, in order to expand the isolation region towards the low frequency, the configurative parameters have to be chosen so that the dimensionless dynamic stiffness at the equilibrium position of the system must be within from 0 to one

5. CONCLUSION

This paper introduced a low frequency vibration isolation model. By expanding

Taylor series up to third order around equilibrium position ($u=0$), the approximated restoring force was obtained. Then, the approximated dynamic equation of the system was also presented. The normal form method is employed to find the steady state response of the system. From this analysis, the vibration transmissibility curve is predicted for the various configurative parameters. The simulation results showed that the vibration isolation effectiveness of the isolator is perfect when the dynamic stiffness at the equilibrium position is nearly equal to zero. However, the limitation of this work is invariant isolation load.

REFERENCES

- [1] Douglas Thorby, *Structural dynamic and vibration in practice*, 401 pages, Elsevier Ltd, 2008.
- [2] S. Graham Kelly, *Fundamentals of mechanical vibrations*, 617 pages, McCraw-Hill, 2002.
- [3] G.S. Paddan, M.J. Griffin, *Evaluation of whole-body vibration in vehicle*, Journal of Sound and Vibration 253 (1) (2002) 195 - 213.
- [4] L.N Virgin, R.B. Davis, *Vibration isolation using buckled struts*, Journal of sound and vibration 260 (5) (2003) 965 - 973.
- [5] E.J. Chnin, K.T. Lee, J. Winterflood, L. Ju, D.G. Blair, *Low frequency vertical geometric anti-spring vibration isolators*, Physics letters A 336 (2-3) (2005) 97 - 105.
- [6] J. Winterflood, T.A. Barber, D.G. Blair, *Mathematical analysis of Euler spring vibration isolator*, Physics letters A 300 (2-3) (2002) 131 - 139.
- [7] R.H. Plaut, H. M. Favor, A.E. Jeffers, L.N. Virgin, *Vibration isolation using buckled or pre-bent columns-part 1: Two-dimensional motion of horizontal rigid bar*, Journal of Sound and Vibration 310 (1-2) (2008) 409 – 420.
- [8] L.N. Virgin, S.T. Santillan, R.H. Plaut, *Vibration isolation using extreme geometric nonlinearity*, Journal of Sound and Vibration 315 (3) (2008) 721 - 731.
- [9] S. Santillan, L.N. Virgin, R.H. Plaut, *Equilibria and vibration of a heavy pinched loop*, Journal of Sound and Vibration 288 (1-2) (2005) 81 - 90.

Corresponding Author:

Le Thanh Danh

Ho Chi Minh City University of Technology

Email: le_thanh_danh@hotmail.com